

# An Investigation on Cooling of CZT Co-Planar Grid Detectors

J. V. Dawson\* C. Montag, C. Reeve, J. R. Wilson, K. Zuber

*Department of Physics and Astronomy, University of Sussex, Falmer, Brighton.  
BN1 9QH UK*

---

## Abstract

The effect of moderate cooling on CdZnTe semiconductor detectors has been studied for the COBRA experiment. Improvements in energy resolution and low energy threshold were observed and quantified as a function of temperature. Leakage currents are found to contribute typically  $\sim 5$  keV to the widths of photopeaks.

*Key words:* CZT, CdZnTe, CPG, Co-Planar Grid, COBRA, double beta decay, energy resolution, threshold

*PACS:* 81.05.Dz, 29.40.Wk, 07.85.-m

---

## 1 Introduction

In recent years a lot of effort has gone into the understanding of new semiconductor materials. There is much industrial and scientific interest in the development of Cadmium Zinc Telluride (CZT) detectors because of their high stopping power and room temperature operation. Such devices have a wide field of application in hard X-ray/ $\gamma$ -ray astronomy, medical imaging applications and general radiation detection like dosimetry.

A novel application is their usage to search for rare nuclear decays. The COBRA experiment is planning to use a large array of Cadmium Zinc Telluride (CZT) semiconductors, to search for neutrinoless double beta decays [1]. Neutrinoless double beta decay, the simultaneous decay of two neutrons inside a nucleus with the emission of two electrons only is not allowed in the Standard

---

\* corresponding author

*Email address:* [jaime.dawson@gmail.com](mailto:jaime.dawson@gmail.com) (J. V. Dawson).

<sup>1</sup> COBRA collaboration: <http://cobra.physik.uni-dortmund.de>

Table 1  
 Double Beta Decay Isotopes present in CdZnTe

Isotope	Q-value keV
$\beta\beta$ emitters	
$^{114}\text{Cd}$	534
$^{116}\text{Cd}$	2805
$^{128}\text{Te}$	868
$^{130}\text{Te}$	2529
$^{70}\text{Zn}$	1001
$\beta^+\beta^+$ emitters	
$^{108}\text{Cd}$	231
$^{106}\text{Cd}$	2771
$^{120}\text{Te}$	1722
$^{64}\text{Zn}$	1096

13 Model of Particle Physics, it requires that a neutrino is its own antiparticle as  
 14 well as that it has a non-vanishing rest mass. For more details see [1].

15 For a double beta decay experiment, CZT offers great potential. Of the 35  
 16 known isotopes able to undergo double beta decay, CZT contains 5 of them  
 17 as shown in Table 1. Of special interest are  $^{116}\text{Cd}$  and  $^{130}\text{Te}$  due to their high  
 18 Q values.

19 Such decays would produce signals due to the combined energy deposit of  
 20 the two emitted electrons. Since no neutrinos are emitted in this process, a  
 21 peak is observed (broadened by the energy resolution of the detectors) at the  
 22 Q-value of each decay. The rate of these events is proportional to the mass of  
 23 the neutrino.

24 For decays in which neutrinos are emitted, the allowed double beta decay  
 25 process, the observed total energy deposits like below the Q-value, forming a  
 26 spectrum similar to that observed from beta decay. The experimental challenge  
 27 is to be able to separate the peak due to the neutrinoless mode from the  
 28 spectrum produced by the more frequent allowed mode. This requires a good  
 29 energy resolution, typically less than 2% at 2.8 MeV.

30 Additionally 4 of the isotopes can also undergo double positron decay, hence  
 31 emitting positrons instead of electrons ( $\beta^+\beta^+$ ) as shown in Table 1. Although,  
 32 due to energy constraints only  $^{106}\text{Cd}$  can emit two positrons, whilst the other  
 33 isotopes decay via mixed modes of positron and single electron capture of a  
 34 K-shell electron ( $\beta^+/EC$ ) and double electron capture ( $EC/EC$ ) modes.

35 For the modes which emit one or more positrons, the resultant signal can also  
 36 comprise one or more 511 keV annihilation photons. In a large array, it is  
 37 possible that the 511 keV photons will be detected a CdZnTe crystal other  
 38 than the one in which the decay occurred. As each crystal signal is read-out  
 39 separately this would be produce two or more coincident triggers, with known  
 40 energy values in each crystal. These coincident signals are characteristic of  
 41 these processes and a powerful search technique.

42 The energy range of the observed events span a wide range from the detection  
 43 of X-rays only from double electron capture (around 60 keV for  $^{106}\text{Cd}$  decay)  
 44 up to a pair of electrons with total energy 2.8 MeV for  $^{116}\text{Cd}$  double beta  
 45 decay.

46 Common to all these decays is the fact that they are very rare, with half-lives  
 47 well beyond  $10^{20}$  years. For the latest COBRA results see [2]. The half-life  
 48 sensitivity of the experiment is highly dependent on the energy resolution of  
 49 the detectors. For the background limiting case, in which one observes no  
 50 events, the lower limit on the half-life  $T^{1/2}$  comes from the Poisson fluctuation  
 51 on the total number of background counts observed within the peak region.  
 52 The lower limit on the half-life  $T^{1/2}$  (years) is:

$$53 \quad T^{1/2} = \ln(2) \cdot \epsilon \cdot N_A \cdot \frac{M}{M_A} \sqrt{\frac{M \cdot t}{\Delta E \cdot B}} \quad (1)$$

54 where  $\epsilon$  is the efficiency,  $N_A$  is Avagadro's number,  $M$  is the mass of isotope  
 55 in kg,  $M_A$  is the atomic mass (kg),  $t$  is the measuring time (years),  $B$  is the  
 56 background rate (events  $\text{kg}^{-1}\text{keV}^{-1}\text{year}^{-1}$ ) and  $\Delta E$  is the energy resolution  
 57 (keV).

58 For a full-scale experiment, with which one would be sensitive to a neutrino  
 59 mass of  $\sim 50$  meV, the mass of isotope required is typically 100 kg. In such an  
 60 experiment, the rate of neutrinoless double beta decays observed may be less  
 61 than a few per year.

62 To detect such low count rates requires a detector and surrounding compo-  
 63 nents of extremely high radiopurity. Shielding from cosmic rays and ambient  
 64 trace radioactive backgrounds is essential. Experiments are sited underground,  
 65 for COBRA in Laboratori Nazionali del Gran Sasso (LNGS, Italy). The lo-  
 66 cal radioactivity is combatted using thick neutron shields and lead castles.  
 67 Detectors are usually housed inside an inner ultra-clean copper shield which  
 68 protects against the trace radioactivity of the lead castle. One possible large  
 69 source of radioactive contamination comes from the detector electronics. For  
 70 the COBRA experiment, like other semiconductor rare search experiments,  
 71 the pre-amplifier electronics are placed outside the lead castle, well separated  
 72 from the inner crystals. This has one obvious drawback, that the detector en-

73 ergy resolution is thus compromised and effectively degraded due to the long  
74 signal cable lengths needed.

75 Other physics searches are also possible such as the second-forbidden unique  
76 electron capture of  $^{123}\text{Te}$  [3,5], which would produce a peak at 30.5 keV. The  
77 group has also performed measurements of the four-fold forbidden non-unique  
78 beta decay of  $^{113}\text{Cd}$  [4] which has a Q-value of  $320\pm 2$  keV [11]. The shape of  
79 the beta decay spectrum is not well predicted by theory, and has only been  
80 observed by a few experiments.

81 To maximise the physics output of the COBRA experiment the ideal energy  
82 range observable by each subcomponent detector is between 25 keV and 3  
83 MeV, with the best possible energy resolution.

84 The current COBRA incarnation is a small R&D array, designed with the aim  
85 of testing the coincident search technqie. It comprises 64 CdZnTe semicon-  
86 ductors of  $1\text{ cm}^3$  organised in a  $4\times 4\times 4$  array. The total mass of the experi-  
87 ment is  $\sim 400\text{g}$ . The crystal support structure is manufactured from delrin,  
88 and placed in a copper shield of 15 cm thick. The surrounding lead shield is 20  
89 cm thick. A narrow slit in the copper shield and a V-shaped lead brick allows  
90 the detector cabling to pass through the shielding layers to the pre-amplifier  
91 electronics.

## 92 1.1 *The Detectors*

93 The COBRA crystals were supplied by EV PRODUCTS, and due to the quan-  
94 tity required and financial constraints, are all low-grade. The crystals were sup-  
95 plied without contacts; ie no wires glued to the electrodes, as all contacting  
96 methods commercially used are not sufficiently radiopure for a low background  
97 experiment. Typical methods of contacting are gluing with conductive epoxy  
98 or soldering. The crystals supplied are exactly the same in electrode design  
99 and size as those purchased pre-contacted and housed.

100 Techniques are sought to improve the energy resolution of this experiment  
101 whilst maintaining the low background. In this paper we consider the effect  
102 of slight cooling of the CZT detectors which could be provided by delivering  
103 cool nitrogen gas, from liquid nitrogen boil off, directly into the heart of the  
104 experiment. This would be a convenient technique since warm nitrogen gas is  
105 already delivered into the crystal housing in order to flush out radon gas.

106 The aim of this paper is to explore the effect of slight cooling of CZT detectors  
107 on energy resolution in general and the improvement for double beta searches  
108 specifically.

109 This work presents a systematic study of the effect of temperature on three  
110 Co-Planar Grid (CPG) crystals all with size  $1 \times 1 \times 1 \text{ cm}^3$  and all manufactured  
111 by eV PRODUCTS, of which two were purchased uncontacted, the COBRA  
112 detectors, and one which was bought commercially.

113 The CPG structure forms a virtual Frisch grid below the anode, and the  
114 resulting signal is produced by electrons travelling past this virtual grid to  
115 the anode. In this way there is almost no position dependence on the signal  
116 amplitude and only the electron signal will be readout [6].

117 It is well known that slight cooling can dramatically reduce leakage currents,  
118 and potentially enhance the observed energy resolution. Temperature effects  
119 on similar sized CPG detectors have previously been reported [8,10], however  
120 in these study the preamplifier electronics were also cooled. Effects on pixel  
121 detectors has also been reported [9].

## 122 2 Experimental Setup

123 For a systematic study of CZT crystal response under slight cooling, two  
124  $1 \times 1 \times 1 \text{ cm}^3$  CZT crystals with gold CPGs produced by eV PRODUCTS were  
125 used. These crystals, designated A and B, were purchased for the COBRA  
126 experiment and setup as follows. The two COBRA CPG crystals are seated in  
127 a delrin holder, with their contacts bonded on to two Kapton cables using a  
128 homemade low radioactivity conductive glue. One Kapton cable supplies the  
129 HV to the cathodes, and one is for the two anode connections (see photograph  
130 Figure 1). The guard rings were not connected. This is the usual manner to run  
131 the detectors for the COBRA experiment as it keeps the active volume large.  
132 The signal cable is  $\sim 30 \text{ cm}$  long. This cable plugs in to COBRA designed  
133 preamplifier and subtraction circuit electronics, based on the recommendation  
134 of eV PRODUCTS

135 All preamplified signals are then shaped by an Ortec 855 shaping amplifier  
136 with a shaping time of  $1 \mu\text{s}$ , digitised by 2048-channel MCA card, and recorded  
137 by computer. The resulting spectra are analysed using ROOT peak finding and  
138 continuum subtracting algorithms (TSpectrum), and the identified photopeaks  
139 fitted with a two-sided Gaussian (with different rising and falling sigmas). The  
140 Full Width Half Maximum is calculated using the average sigma. A full sweep  
141 of all parameters; CPG balance potentiometer, grid bias and cathode voltage,  
142 was made for both crystals with  $^{137}\text{Cs}$  spectra recorded for each combination.  
143 The shaping time was not optimised and remained at  $1 \mu\text{s}$ . The optimum pa-  
144 rameters for each crystal are those settings at which the best energy resolution  
145 of the 662 keV photopeak was seen at room temperature.



Fig. 1. The COBRA setup with 1 crystal. 16 crystals can be placed in to the Delrin holder. HV Kapton cable contacts to the cathode, and signal Kapton cable contacts the anodes.

146 The COBRA crystal holder was placed in a temperature controlled copper box,  
 147 with a narrow slit to allow the Kapton cables to pass through. The copper  
 148 box acts as a Faraday cage. An external peltier cooler is in close thermal  
 149 contact with the exterior of the box. The thick copper walls (3 mm) produce  
 150 a even thermal bath which is monitored by two temperature sensors inside.  
 151 The peltier itself is cooled by a closed-loop pumped water system and cooling  
 152 fans. The fan system produces a significant amount of noise which degrades the  
 153 energy resolution of the detectors. Since the copper box is significantly massive,  
 154 the fan system is switched off during the measurement and the temperature  
 155 monitored to ensure stability during the measurement. The measurements  
 156 are therefore relatively short, of 100 s duration, but are repeated to ensure  
 157 repeatability. The temperature range of interest is from 2°C to 20°C.

### 158 3 Resolution Function of a Commercial Detector

159 All CPG detectors show a linear increase in Full Width Half Maximum with in-  
 160 creasing energy. A possible explanation for this trend could be from the coplanar  
 161 grid. Whilst the CPG design counteracts the effect of the hole-trapping  
 162 in CdZnTe, the electrode design may also limit the resolution [7]. An x-y scan  
 163 was made across the cathode surface of a commercial eV PRODUCTS de-  
 164 tector with a collimated 60 keV source. The detector was a 1 cm<sup>3</sup> detectors,  
 165 bonded to eV PRODUCTS preamplifier and subtraction circuit, and housed  
 166 in a cylindrical aluminium casing. We observed a systematic linear change in  
 167 the photopeak position of the 60 keV line along one axis of  $\sim 5\%$ . This effect  
 168 was first reported in [7]. Illuminating the whole cathode of the detector results  
 169 in a wider photopeak due to this effect.

170 Another important source of resolution broadening is the fluctuation of the  
 171 leakage current. For these detectors, however, we find that leakage current is

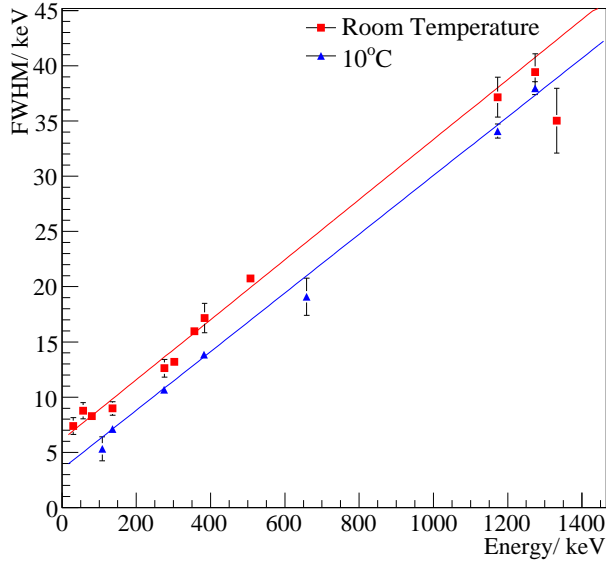


Fig. 2. Resolution Function for commercial detector at 22°C and 10°C

172 only significant for low energy events (below a few hundred keV).

173 A clear improvement was observed by cooling the commercial eV PRODUCTS  
 174 detector as shown in Figure 2. This clearly shows the linear dependence of  
 175 the FWHM with energy. Results are shown for measurements made at room  
 176 temperature for incident gamma rays and with the entire device (crystal and  
 177 pre-amplifier electronics) cooled to 10°C. Cooling this detector results in a  
 178 15% improvement at 500 keV, and a 5% improvement at 2.8 MeV. The shift  
 179 downwards in intercept and overall performance improvement is interpreted  
 180 as due to the reduction of bulk, surface leakage currents and electronic noise.

## 181 4 COBRA CZT Crystals

182 After the encouraging results from the commercial detector the COBRA crys-  
 183 tals were cooled, with the preamplifier electronics remaining at room temper-  
 184 ature (23°C). No spectral change was observed for the photopeaks of  $^{22}\text{Na}$   
 185 (511 and 1254 keV),  $^{137}\text{Cs}$  (662 keV) and  $^{60}\text{Co}$  (1173 and 1332 keV). However,  
 186 improvements were observed with  $^{241}\text{Am}$  (60 keV) and  $^{57}\text{Co}$  (122 keV).

### 187 4.1 Low Energy Response

188 Low energy spectra show a significant enhancement in resolution under cool-  
 189 ing. Figures 3 and 4 show the spectral change observed for  $^{241}\text{Am}$  and  $^{57}\text{Co}$

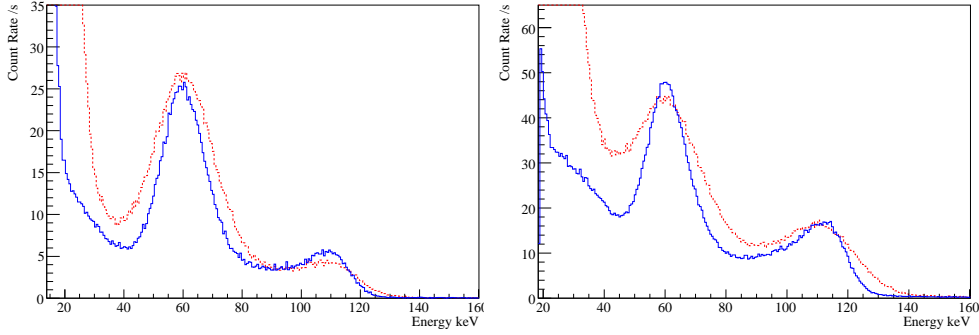


Fig. 3.  $^{241}\text{Am}$  spectrum of crystal A (left) and B (right) at room temperature ( $23^\circ\text{C}$ ) (dashed line) and under cooling ( $5^\circ\text{C}$ )(solid line). The feature to the right of the 60 keV peak is due to multiple events.

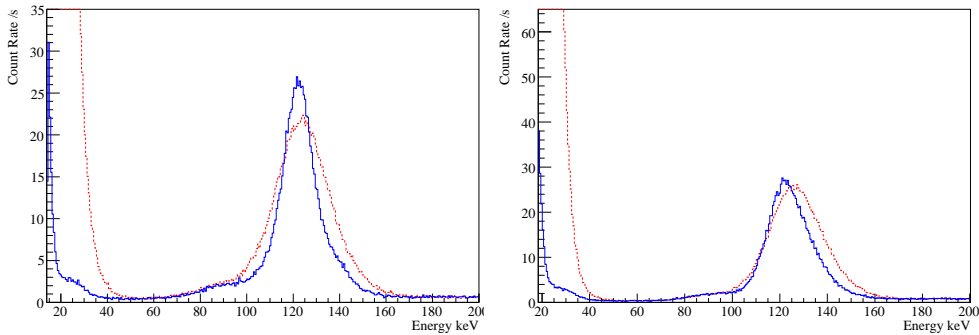


Fig. 4.  $^{57}\text{Co}$  spectrum of crystal A (left) and B (right) at room temperature ( $23^\circ\text{C}$ )(dashed line) and under cooling ( $5^\circ\text{C}$ ) (solid line).

190 sources cooled to  $5^\circ\text{C}$  . A clear improvement is observed with cooling; the pho-  
 191 topeaks become narrower such that other spectral features become visible. In  
 192 addition, the low energy threshold drops such that features at 30 keV become  
 193 apparent.

194 Measurements of the FWHM of the 122 keV line from  $^{57}\text{Co}$  and the 60 keV line  
 195 from  $^{241}\text{Am}$  were made as a function of temperature for the two crystals, and  
 196 are shown in Figures 5 and 6. The sources were not collimated and the cathodes  
 197 of both detectors were equally illuminated. Both data sets are fitted by a single  
 198 exponential function combined with a constant offset. The exponential form  
 199 of the fitted function represents the magnitude and response of the crystal to  
 200 temperature. Supporting this, the resulting fit parameters of the 60keV and  
 201 122keV lines are compatible for each individual crystal, but not compatible  
 202 between crystals i.e. the temperature response is a detector property.

203 The leakage current is reduced such that it is insignificant compared to other  
 204 sources of photopeak broadening. For crystal A, the leakage current component



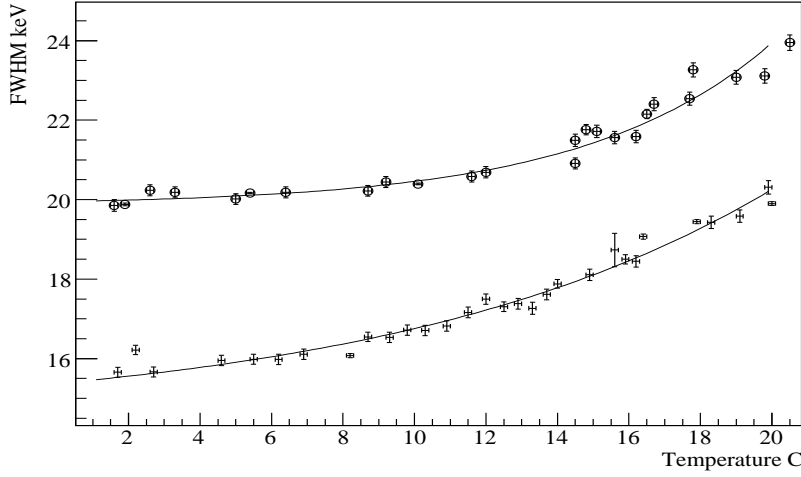


Fig. 5. Change in the FWHM of the 122 keV line of  $^{57}\text{Co}$  as a function of temperature for crystals A(circles) and B(points). Fits to A:  $(19.84 \pm 0.03) + (0.10 \pm 0.01)e^{(0.185 \pm 0.009)T}$  and B  $(14.6 \pm 0.2) + (0.8 \pm 0.1)e^{(0.097 \pm 0.007)T}$ .

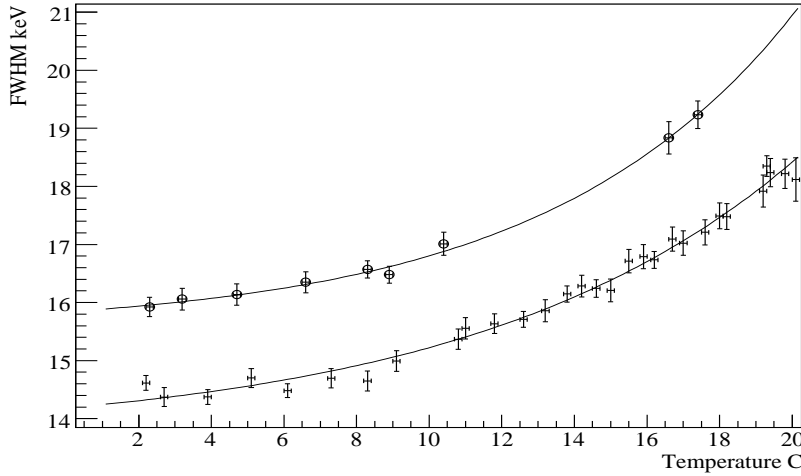


Fig. 6. Change in the FWHM of the 60 keV line of  $^{241}\text{Am}$  as a function of temperature for crystals A(circles) and B(points). Fits to A:  $(15.5 \pm 0.3) + (0.3 \pm 0.2)e^{(0.15 \pm 0.04)T}$  and B  $(13.7 \pm 0.2) + (0.5 \pm 0.1)e^{(0.11 \pm 0.01)T}$

205 of the FWHM is  $lc(T)_A = (0.10 \pm 0.01)e^{(0.185 \pm 0.009)T}$  and for crystal B  $lc(T)_B =$   
 206  $(0.8 \pm 0.1)e^{(0.097 \pm 0.007)T}$ .

207 The residual FWHM comes from other components unaffected by temper-  
 208 ature such as electronic noise, cable length, detector performance, and any  
 209 geometrical broadening.

210 Cooling to  $5^\circ\text{C}$  brings a 25% improvement to the resolution of the 122 keV line  
 211 on crystal A and 22% improvement on crystal B. For these crystals further

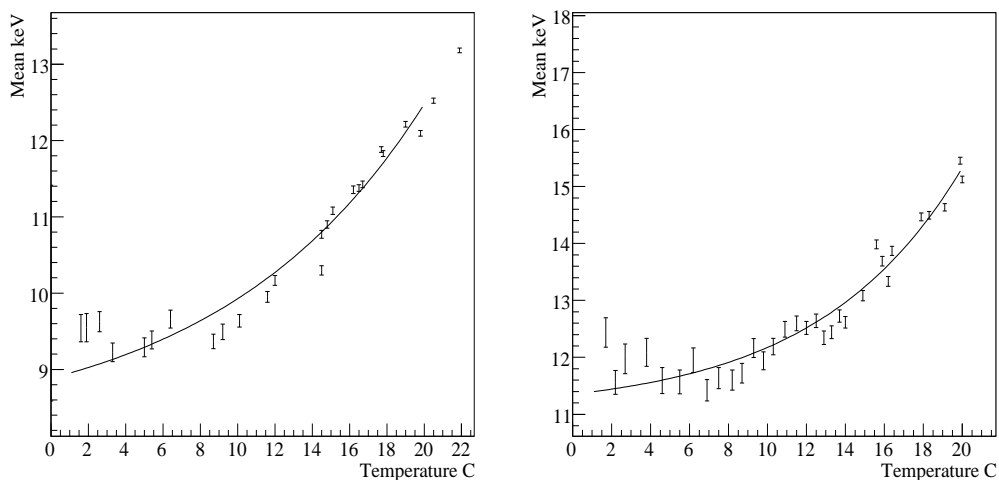


Fig. 7. Variation of the Poisson mean of the pedestal as a function of temperature from crystal A (left) and B(right).

212 cooling will not bring significant improvements to the energy resolution.

#### 213 4.2 Low Energy Thresholds

214 Cooling the CZT crystals results in a significant improvement in lower energy  
 215 threshold due to the reduction in leakage current, with the pedestal feature  
 216 observed in the spectra clearly reducing in size. Poisson fits to the pedestal  
 217 were made for spectra from both crystals for different temperatures. Figure 7  
 218 shows how the fitted mean reduces with temperature. Additionally the height  
 219 of the noise pedestal also diminishes as shown in Figure 8. Similar to the  
 220 photopeak resolutions, the energy threshold reaches a minimum value at  $\sim 5^\circ\text{C}$   
 221 and further cooling does not improve the threshold.

222 In rare search mode, the low energy threshold is always far greater than that  
 223 observed during calibrations with a high rate source. The low energy threshold  
 224 can be thought of as the energy at which the noise rate drops below the  
 225 real physics event rate. Low rate searches therefore experience higher low  
 226 energy thresholds. Whilst it is possible to observe low energy lines  $\sim 30$  keV  
 227 during calibrations, the low energy threshold is often  $\sim 50$  keV or higher in  
 228 low background operation.

229 The energy threshold is therefore defined to be the energy at which the noise  
 230 rate falls below a pre-determined value. Using the results of the Poisson fit  
 231 to the noise pedestal (shown in Figures 7 and 8) for a particular operating  
 232 temperature, one can find the energy at which the noise rate falls below a  
 233 given value. For example, for a desired threshold event rate of  $10^{-4}$  Hz at  
 234  $23^\circ\text{C}$  crystal A would have a low energy threshold of 37.6 keV. Lowering the

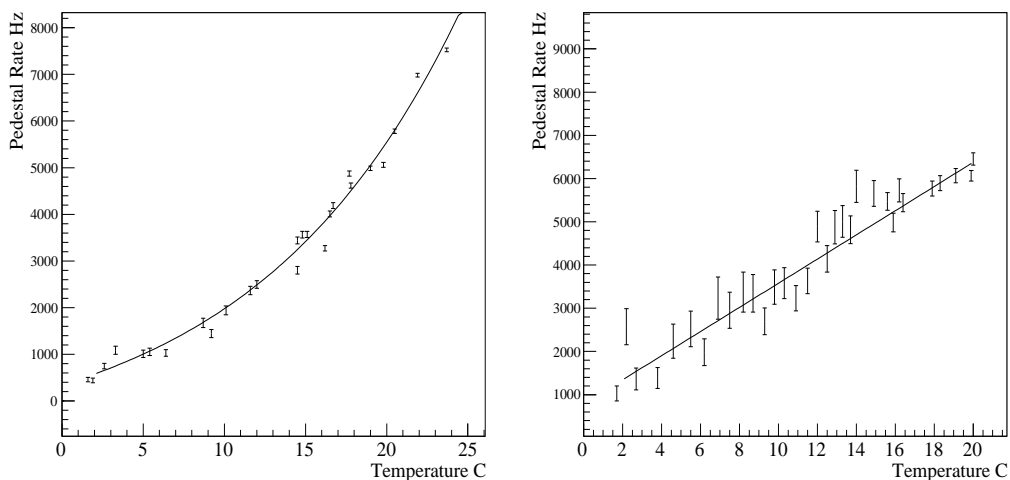


Fig. 8. Variation of the number pedestal counts as a function of temperature from crystal A (left) and B(right).

235 temperature to  $5^{\circ}\text{C}$ , would reduce this threshold to 29.1 keV. Similarly for  
 236 crystal B, the low energy threshold would be 41.8 keV at room temperature  
 237 reducing to 33.8 keV with cooling.

## 238 5 Resolution Function

239 Figure 9 shows the resolution functions observed with the two crystals A and  
 240 B. Since no spectral change was observed for these two crystals for the higher  
 241 energy lines (511 keV and above), the two straight lines above the 511 keV  
 242 point represent the trend for both room temperature and under cooling. For  
 243 the lower energy lines, the trends differ and the same linear trend is no longer  
 244 followed. This illustrates how temperature affects the resolution function. This  
 245 also shows how determining the resolution function using high energy lines  
 246 and extrapolating to lower energies may result in a wrong determination of  
 247 the widths of the low energy lines.

248 The behaviour of the resolution of the two COBRA crystals is different to that  
 249 of the commercial detector, as shown in Figure2, where the room temperature  
 250 and cooled resolution functions are well separated and virtually parallel. In  
 251 the COBRA case there is no discernable difference between the room temper-  
 252 ature and cooled resolution functions at 511 keV. Here the derived resolution  
 253 functions merge with FWHMs of  $\sim 35$  keV. This resolution is only reached  
 254 for the highest energy lines observed with the commercial detector and we  
 255 assume that for higher energy lines the resolution functions would also begin  
 256 to merge.

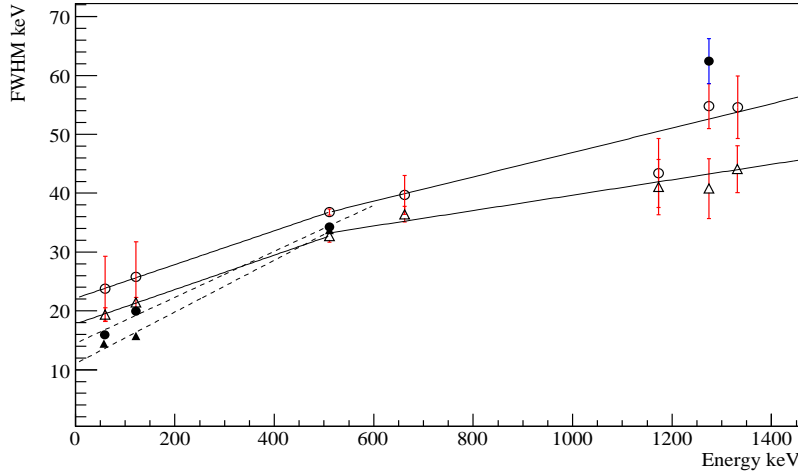


Fig. 9. FWHM versus energy for crystals A (circles) and B (triangles), open and filled markers denote room temperature and cooled data respectively. The solid lines show the trend from the 511 keV line and above. Below this the 511 keV line the trends change, solid represents the room temperature results and the dashed line is with maximum cooling (no leakage current).

257 For better-performing commercial detector the leakage current is a major  
 258 source of broadening across the range 60 to 1300 keV. For the COBRA de-  
 259 tectors, the leakage current component is less important with respect to the  
 260 the other sources of broadening such as the electronic noise. For the COBRA  
 261 detectors the electronic noise term is higher and therefore the leakage current  
 262 is less significant. For energies above  $\sim 300$  keV the leakage current is insignifi-  
 263 cant with respect to the other sources of broadening. Therefore to improve the  
 264 resolutions of higher energy lines, methods to counteract this other component  
 265 must be found.

## 266 6 Conclusion

267 A systematic study of the behaviour of two CZT Co-Planar Grid crystals  
 268 under moderate cooling has been made. Significant improvements in photo-  
 269 peak resolution and low energy thresholds were observed. A temperature of  
 270 only  $5^\circ\text{C}$  was found to be sufficient, below this no further improvement was  
 271 observed.

272 The change in FWHM of photopeaks as a function of temperature was found  
 273 to be well fitted by an exponential trend. For each crystal, the 60 keV and  
 274 122 keV datasets were fitted to this exponential function and the resulting fit  
 275 parameters were found to be compatible, i.e. the behaviour of the photopeak  
 276 resolution with temperature is the same for all energies. This is interpreted as

277 leakage current decreasing with decreasing temperature.

278 Both crystals exhibit  $\sim 21\%$  and  $\sim 16\%$  improvement in resolution at 60 keV  
279 and 122 keV respectively under cooling. Improvements at higher energies  
280 above  $\sim 300$  keV are indiscernable, due to the insignificance of leakage current  
281 broadening at these energies. The resolution here is thought to be dominated  
282 by geometric and electronic effects. Typically leakage currents are found to  
283 contribute  $\sim 5$  keV to the widths of photopeaks. For these two crystals, other  
284 noise sources which are not affected by the temperature of the crystal, such as  
285 the electronic noise, contribute a large part of the FWHM of the photopeaks.  
286 It is clear that the reduction of this contribution will be beneficial.

287 The resolution functions, trend of FWHM with photopeak energy, have been  
288 determined for the commercial eV PRODUCTS detector and the two COBRA  
289 detectors. They both show linear increases in FWHM as a function of energy.  
290 This is interpreted as being a geometric effect, where energy depositions on  
291 one side of the detector give systematically large signals than the opposing  
292 side. Under cooling, the commercial detector shows improvements from 60 to  
293 1300 keV. For the highest energy lines observed with the commercial detector  
294 the FWHMs are  $\approx 35$  keV. With the COBRA detectors this FWHM is reached  
295 at a lower energy at 511 keV. Above this there is no improvement seen with  
296 the cooling as the leakage current is not the dominant source of broadening.

297 Moderate cooling reduces the low energy threshold due to the reduction in  
298 leakage current. We consider a low background threshold event rate of  $10^{-4}$  Hz,  
299 such that the COBRA experiment operates at, and show that cooling would  
300 reduce the experimental threshold of these detectors by  $\sim 20\%$ , to 30 and 34  
301 keV for crystals A and B. We consider that cooling the crystals to  $5^\circ\text{C}$  of the  
302 already running COBRA experiment would bring about similar improvements.  
303 This would allow a search for the second-forbidden unique electron capture of  
304  $^{123}\text{Te}$ , peak at 30.5 keV.

305 For the present COBRA experiment, mild cooling will improve the physics  
306 search sensitivity to low energy lines only and will bring no improvements to  
307 the search for high energy lines. However, the improvements in low energy  
308 threshold increase the physics reach of the experiment.

309 To improve the resolution on the high energy lines, such as  $^{116}\text{Cd}$  2.8 MeV  
310 line, work should focus on investigating and reducing the broadening effects  
311 which are dominant at this energy. This currently appears to be due to the  
312 design of the CPG grids and the pre-amplifier electronics. Future work will  
313 also concentrate on reducing the electronic noise, with the aim of pushing the  
314 low background threshold to well below 30 keV.

315 **References**

- 316 [1] K. Zuber, *Physics Letters B* **519** (2001) 1.
- 317 [2] T. Bloxham et al, *Physical Review C* **76**(2007) 025501.
- 318 [3] D Münstermann et al, *J. Phys. G: Nucl. Part. Phys.* **29** (2003) B1-B4.
- 319 [4] C. Gössling et al, *Physical Review C* **72**, 064328 (2005).
- 320 [5] Alessandrello et al, *Phys. Rev. C* **67** (2003) 014323.
- 321 [6] P. Luke, *IEEE Trans. Nucl. Sci.* **42** (1995) 4.
- 322 [7] He Z., Sturm B. W., *Nuc. Inst. Meth. in Phys. Res. A* **554** (2005) 291.
- 323 [8] Sturm B. W., He Z., *IEEE Trans. Nucl. Sci.* **52** (2005) 2068.
- 324 [9] Yadav J. S., Savitri S., Malkar J. P, *Nuc. Inst. Meth. in Phys. Res. A* **552**  
325 (2005) 399-408.
- 326 [10] Amman M, Lee J. S., Luke P.N, *IEEE Trans. on Nuc. Sci.* **53** (2006) 3035.
- 327 [11] The 8th edition of the Table of Isotopes, Richard B. Firestone, Virginia S.  
328 Shirley, Coral M. Baglin, S.Y. Frank Chu, and Jean Zipkin. John Wiley & Sons  
329 Inc., 1996.